The Impact of The Preventive Role of Star Anise on The Toxicity of Benzopyrene Compound in The Liver and Kidney Tissues and Biochemical Parameters in Male Rats

Eman Naji Saleh[1] , Iktefa Abdul Hamid Mohammed Saeed[2] , Nedhal ibrahim latef[3]

[1]*Department of biology, College of Education for Pure Sciences ,University of Anbar, Iraq. And University Of Tikrit, Tikrit,Iraq Email: aemanng349@uoanbar.edu.iq*
[2]*Biology Department, Education College for Women, University Of Tikrit, Tikrit,Iraq*
[3]*College of Education for women, University of Anbar, Iraq*

KEYWORDS
Benzopyrene, liver, kidney, biochemical, histopathology

ABSTRACT
Objective: This study, conducted at the University of Anbar's College of Pure Science, evaluated the protective effects of star anise against benzopyrene (B[a]P)-induced liver and kidney damage in 30 male white Swiss rats (Sprague Dawley), aged 3-4 months and weighing between 170-210 g. Materials and methods: The rats were divided into six groups: Control (G1), B[a]P (G2), Star Anise 125 mg/kg bw (G3), Star Anise 120 mg/kg bw + B[a]P (G4), Star Anise 125 mg/kg bw + B[a]P (G5), and Star Anise 130 mg/kg bw + B[a]P (G6). Results:Biochemical analyses showed that B[a]P exposure significantly elevated liver enzymes (ALP, AST, ALT, GGT) and kidney markers (uric acid, creatinine), indicating hepatic and renal damage. Treatment with star anise, especially 130 mg/kg bw significantly reversed these elevated levels because it protected against the injury. Histopathology showed that the liver and kidney were severely damaged in the B[a]P group and in the star-anise-treated group, normal tissue architecture was well preserved only in high doses of star anise treatment. Conclusion:These outcomes suggest the use of star anise as a hepatoprotective as well as a nephroprotective agent, and this needs to be further strengthened by understanding its mechanisms and long-term effectiveness.

1. Introduction

Benzopyrene (B[a]P) is an environmental hazard and a carcinogen of concern given its association with cancers of the lung, liver, and kidney. It is a component of tobacco smoke, vehicle exhaust, and charcoal-grilled foods, and thus is a major risk factor for people exposed to it. Its toxicological effects include inducing oxidative stress, DNA damage, and cellular dysfunction as a result of accumulating B[a]P in target organs and/or tissue. B[a]P promotes the generation of reactive oxygen species (ROS) that can cause oxidative damage to proteins, lipids, and DNA.B[a]P alters redox balance, features of cancer, aging, oxidative stress, and neurodegenerative disease. Reactive oxygen species are one reason for B[a]P-induced damage and toxicity. B[a]P leads to covalent binding to nuclear receptors- and other proteins, which results in genomic and non-genomic effects. Yet, the biotransformation that occurs in the liver through the action of the drug-metabolizing enzymes may result in the formation of ROS as well as B[a]P diol epoxides – highly reactive semi-saturated metabolites, which have been shown to attach to DNA nearly 100 times more frequently than the parent molecule B[a]P. The cytochrome P450 enzymes, particularly CYP1A1, CYP1A2, and CYP1B1, are responsible for the metabolism of B[a]P into reactive intermediates, including B[a]P-7,8-diol-9,10-epoxide, which then binds to DNA leads to an alteration in cellular DNA, called 'DNA adducts', which in turn leads to mutations. Similarly, as does the liver, the kidneys metabolize B[a]P to ROS, which brings about oxidative damage. This secondary oxidative stress can lead to the activation of inflammatory cascades that can result in kidney injury (1). B[a]P metabolites can also form DNA adducts in renal cells. This could lead to a change in the nucleotide base sequence – what we call mutations – which could lead to renal carcinogenesis (2). Acute and chronic B[a]P exposure can impair renal function. Serum biomarkers such as creatinine, blood urea nitrogen (BUN), and urinary concentrations change to altered levels. Natural antioxidative and cytoprotective compounds were investigated as potential protectors of B[a]P-induced toxicity. Star anise (Illicium verum Hook.f.) is a plant used as a culinary spice and herbal drug. It contains bioactive compounds such as flavonoids and terpenoids that have been shown to reduce oxidative stress and to prevent and eliminate xenobiotics, which are poisons existing in plants, animal by-products, heavy metals, pesticides, etc. A few years ago, numerous in vivo studies demonstrated its numerous health-related pleiotropic activities like anti-inflammatory and anticancer properties. One of these compounds is represented by Quercetin, a natural and valuable flavonoid found in fruits and vegetables, that inhibits the oxidative damage induced by B[a]P. (3)

The administration of plant-derived products like star anise extract is a promising approach for the investigation of preventive strategies against cancer-causing compounds like B[a]P. Some preclinical clues suggest that star anise prevention is a protective model against oxidative stress and tissue injuries, making it potentially useful as a natural component in detoxification and as a cytoprotective agent. However, more in-vivo studies need such protection and test it in experimental models of oxidative stress. (4) The objective of this study was to explore whether star anise extract could prevent the potent toxicity of B[a]P via treating both positive control and experimental exposure to B[a]P of spotted male rats (5). This article assessed our experimental design with six groups: negative control, positive control, positive control with 500 mg kg-1 star anise extract, positive control with 1000 mg kg-1 star anise extract, positive control with 1500 mg kg-1 star anise extract, and positive control with 2000 mg kg-1 star anise extract. Our study elaborated on the protective efficacy of star anise extract as it curbs oxidative damage caused by B[a]P carcinogen in different organs of the males of this species. From our laboratory, biochemical analyses and histopathological examinations will further measure relevant markers of oxidative stress, liver function, kidney health, and neuronal integrity. (6)

It also helps to close the gap between traditional herbal medicine and modern toxicology by adding insight into natural compounds such as star anise that could potentially reduce the health risks associated with environmental pollutants such as B[a]P.

2. Materials and Methods

Experimental design

For this study, table-1 depicted male white Swiss rats (Sprague Dawley) as shown in table-1, aged between 3-4 months old weighing 170-210 g. Rats were placed in plastic cages 15x20x30 cm with metal covers prepared specially for this purpose in the animal house of the Department of Biology/ College of Education for Pure Sciences/ University of Anbar. The animals were subjected to laboratory conditions of a light period divided into 11 hours of light and 13 hours of darkness. The temperature was fixed at 22±2 C. Care was taken to clean the cages and sterilize them every week, where they left for two weeks to adapt to the new conditions and ensure they were free of diseases. Besides, the experimental protocol was approved by a Scientific Research Ethics Committee at College of Veterinary Medicine, University of Fallujah by 27 in 30 /1 /2024

Table 1: animal Grouping

Grouping		Treatment
G1	**-ve Control**	Rats receiving standard diet and water ad libitum.
G2	**B[a]P Group**	Rats exposed to B[a]P for two weeks
G3	**Star Anise Group (25 mg**	Rats were treated via oral gavage once daily for a full month and then exposed to B[a]P for two weeks
G4	**Star Anise (20 mg) + B[a]P Group**	Rats treated with star anise extract (120 mg/kg body weight) via oral gavage once daily for a full month and then exposed to B[a]P for two weeks
G5	**Star Anise (25 mg) + B[a]P Group**	Rats treated with star anise extract (125 mg/kg body weight) via oral gavage once daily for a full month and then exposed to B[a]P for two weeks
G6	**Star Anise (30 mg) + B[a]P Group**	Rats treated with star anise extract (130 mg/kg body weight) via oral gavage once daily for a full month and then exposed to B[a]P for two weeks

Preparation of Star Anise Extract:

Star anise seeds were procured and authenticated. The extraction was carried out using ethanol as a solvent following standard procedures. The extract was concentrated using a rotary evaporator and stored at -20°C until further use. Star anise extract was administered to one group via oral gavage needle for one month. After one month, rats were orally dosed with B[a]P for two weeks to ensure the same exposure to the toxicant in both groups.

Preparation of Benzopyrene (B[a]P):

The chemical, benzopyrene (B[a]P), was prepared as an oral gavage stock used for the experimental groups where high-purity benzopyrene powder, obtained from a third-party accredited chemical supplier, was dissolved in a pharmaceutical-grade olive oil to the corresponding concentration. [7] To keep the solution stable and contamination-free, the preparation was made in reduced light and mixed on a magnetic stirrer, and then placed into amber glass vials and stored at -20°C prior to use. Since the solution contained 2 pmol/µL B[a]P, it gave us sufficient stability until we could use it. These protocols are now common practice in preparing solutions for experiments. This is the secret to what happens to the pollutants in our environment that resist traditional methods of chemical analysis. Each mouse also received a separate administration of B[a]P solution every other day for a total of 10 administrations: for oral administration, the dose of B[a]P solution was thawed at 4 °C overnight and then adjusted to room temperature before subsequent administration. After each administration, the thawed doses of B[a]P solution were injected into stomach of Mice while paying attention to the accuracy of the doses and aseptic technique in the feeding operation, reducing variability and allowing all the exposed groups of the treated groups to show consistent results.

Sample Collection:

We performed histological investigations on liver, kidney, tissues that were removed after the rats were euthanized. The tissues were then washed in ice-cold saline.

The Aspartate Aminotransferase (AST), Alanine Aminotransferase (ALT), and Gamma-glutamyl transpeptidase (GGT)

Blood was collected from the tail vein of experimental rats (Parasuraman et al., AST and GGT enzymes present in rat serum were measured by assay kits (Albumin NH45) delivered from the US company Abcam. The assay protocol provided by them was strictly followed. Briefly, microplates were prepared according to the kit guidelines with ALT, AST standards to mark curves. Samples were added, and ALT, AST and GGT standards were introduced followed by incubation for the stipulated period of time. Absorbance were read using a spectrophotometer. ALT, AST and GGT concentrations were interpolated using the respective curves. ALT, AST and GGT ratio were calculated.

Uric acid and creatinine

Steps of estimating Uric acid and creatinine levels by spectrophotometer (in ratio model)

Blood samples from the Lab rats were collected and seperated the serum to conduct the enzyme activity.

The spectrophotometer is used to find the activity of the enzymes by considering the specific wavelength selected to estimate. The protocols were already established and were then adjusted for rat samples (8,9).

The calculated concentration of Uric acid and creatinine levels were estimated by using the spectrophotometer.

Quality control processes were applied to ensure the accuracy of the results, where each time the reference ranges of the laboratory are set on rato samples (10).

Histological variables

Histopathological changes in the liver and kidney tissues of all experimental animals were evaluated. The rats were dissected, and then the liver was taken and preserved in 10% formalin to fix the tissues. They were then passed through ascending stages in an ethanol solution, thinned with xylene, and Imbibited and embedded in paraffin cubes. After that, thin sections (5–7 µm) were stained with hematoxylin and eosin (H&E) solution and examined under a compound light microscope equipped with a digital camera.

Statistical analysis

The data was assessed using SPSS compute utility 16.0 one-way ANOVA analysis; the $p \leq 0.05$ level was considered to be significant (11).

Results and Discussion

Table 2: liver and kidney functions

	ALP (U/L)	AST (U/L)	ALT (U/L)	GGT (U/L)	Uric acid (mg/dl)	Creatinine (mg/dl)
Control G1	221±2.58D	124.1 ±3.57D	34.13±1.26D	9.21±1.31D	1.04±0.01D	0.381±0.02D
Benzopyrine G2	302±13.75A	201.1±15.50A	56.81±2.84A	36.15±3.58A	1.68±0.27A	0.48±0.019A
Star anis 125 mg\kg bw. G3	221.7±1.53D	123.6 ±1.48D	33.98±1.04D	9.09±1.18D	1.02±0.02D	0.386±0.01D
Star anis 120 mg\kg bw. + benzopyrine G4	281.9±11.06B	178.1±7.91B	46.61±3.77B	20.17±2.32B	1.42±0.11B	0.45±0.03B
Star anis 125 mg\kg bw. + benzopyrine G5	258.1±8.59C	153.7±12.85C	40.45±4.12C	14.84±1.66C	1.31±0.16C	0.42±0.07C
Star anis 130 mg\kg bw. + benzopyrine G6	229.6±12.73D	127.2±7.37D	35.3±2.36D	10.39±3.46D	1.12±0.39D	0.39±0.04D

ALP (Alkaline Phosphatase) levels are significantly elevated in the benzo[a]pyrene (B[a]P) group, compared with other groups, reflecting liver and bile duct stress (12). In Table 2, elevated ALP levels indicate damage or obstruction in the liver or bile ducts, which aligns with the toxic effects of B[a]P. Treatment with star anise, particularly at the highest dose of 130 mg/kg bw (G6), significantly reduces ALP levels, indicating a protective effect on liver function. This observation is consistent with previous research showing that star anise can help maintain liver health by reducing oxidative stress and inflammation (13). In addition, AST levels increased significantly with the [B]aP exposure which is a marker of liver or even cardiac muscle damage (14). AST activity is a marker of hepatocellular injury. The 120, 125, and 130 mg lowered these levels in a dose-dependent manner, treated with 130 mg/kg). Star anise thus exhibited a hepatoprotective effect, consistent with the protective role of the liver against damage or damage induced by lipid peroxidation via antioxidant actions, as shown in the literature (15).

Table 2–The ALT (Alanine Aminotransferase) levels in Grp. Bap(G2) is significantly higher than in other groups, confirming that the mouse model developed liver damage, due to a provoked immune response(16). ALT is a specific marker for liver injury. The reduction of ALT levels by star anise treatment, especially at higher doses, suggests that star anise helps mitigate liver damage caused by B[a]P. The highest dose brings ALT levels closer to those of the control group, supporting the protective effect of star anise on the liver, as previously reported (17). Also, GGT (Gamma-Glutamyl Transferase), an indicator of liver stress, is significantly elevated in the B[a]P group (G2), reflecting hepatic damage (18). Elevated GGT levels indicate oxidative stress and potential damage to the liver's detoxification pathways. Star anise treatment decreases GGT levels, with the highest doses showing the most significant reduction. Other groups also showed significant differences (G4 and G5) and the ability to reduce the toxic effect of benzo[a]pyrene. This suggests hepatoprotective properties of star anise, likely due to its antioxidant activity. This finding aligns with research indicating that star anise beneficially affects liver enzymes by mitigating oxidative damage (19).

Uric acid level would increase two- fold in benzo[a]pyrene treated (G2) (Table2) due to either increased purine metabolism or decreased urinary excretion(20). Highest incidence would be noted at 30mg\kg bw dose of benzo[a]pyrene (Figure 1). Urinary uric acid level appeared to decrease significantly in the treatment groups receiving Star anise compared with control group, especially more pronounced at higher dose 130mg\kg bw. The effect of Star anise in decreasing uric acid level suggests its activity to counteract the oxidative stress and preserve renal functions. This supports the reported antioxidant activity of Star anise (21). The results showed significant difference among the

groups and demonstrated the effectiveness of Star anise to relieve the renoprotective effect of benzo[a]pyrene in kidney function.

Whilst the benzo[a]pyrene group (G2) have significantly higher creatinine levels -an indicator of kidney stress or damage (22) , star anise at the highest dose (130 mg/kg bw) brings down the levels closer to that of control. This could be due to the supposed protective effect of star anise, which has been reported to possess antioxidant properties (23) (Table 2).

Histopathological variables

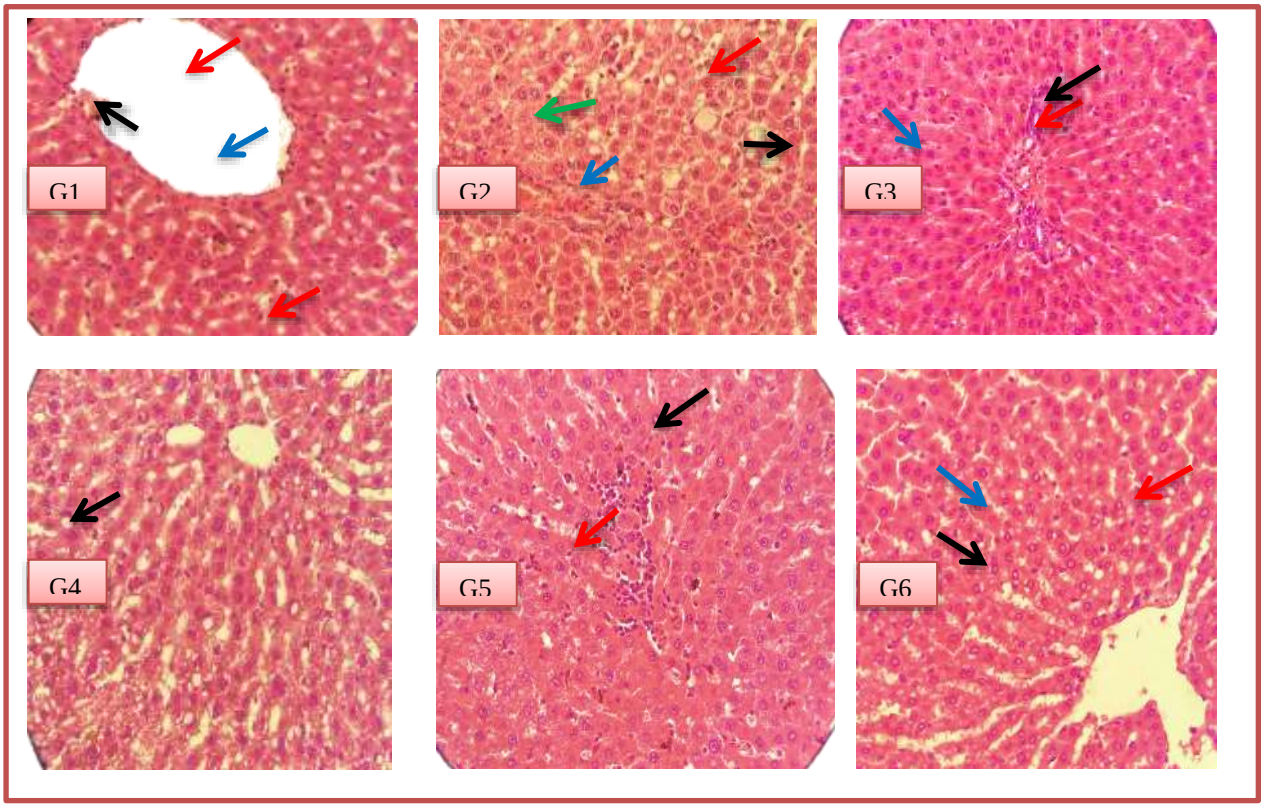

Figure (1) liver tissue :**: (G1)** control group with normal liver tissue, the central vein is observed to have a wide lumen and is lined with simple squamous cells. The rows of polygonal hepatocytes are clearly noted, along with the hepatic sinusoids containing Kupffer cells. This observation is based on H&E staining at a magnification of X40.**: (G2)** In the liver tissue, the blood sinusoids are observed in the form of pockets (A). There is hyperplasia of Kupffer cells in the blood sinusoids (B), atrophy of some hepatocytes (C), and blood congestion in some of the blood sinusoids (D).**: (G3)** The liver tissue is normal, showing a branch of the portal vein (A), bile canaliculi (B), and rows of hepatocytes with dark spherical nuclei (C).**: (G4)** The liver tissue image shows the central vein (A). Some hepatocytes exhibit vacuolar cytoplasmic degeneration (B).**: (G5)** The liver tissue shows rows of uniform hepatocytes (A) and focal infiltration of white blood cells between the hepatocytes (B).**:(G6)** The liver tissue is normal, featuring the central vein (A) connected to the blood sinusoids at its edges, which contain Kupffer cells (B). The rows of hepatocytes are radially organized, each with spherical nuclei, and the cells appear polygonal .

In this study,fig.(1) the histological examination of liver tissues across different treatment groups revealed significant insights into the effects of benzopyrine and the potential protective role of Star Anise. The liver tissue of the control group (G1) exhibited a normal architecture, with a central vein characterized by a wide lumen lined with simple squamous cells. Rows of polygonal hepatocytes were clearly noted, and the hepatic sinusoids contained Kupffer cells. In the liver tissue of the benzopyrine-treated group (G2), significant structural changes were observed. The pockets of blood sinusoids were accompanied by hyperplasia of Kupffer cells where some hepatocytes were atrophied and some sinusoids had blood congestion. These are

indicative of severe disruption of normal architecture liver cells exposed to benzopyrine, which is consistent with previous published data on the hepatotoxic effects of benzopyrine. (24). In the Star Anise 125 mg/kg bw treatment group (G3), the liver tissue had a normal histological appearance including a branch of the portal vein, another bile canaliculi and closely arranged hepatocytes with dark-stained spherical nuclei indicating normal liver tissue. These results suggest Star Anise did not evoke liver damage, consistent with the suggested safe dose of Star Anise reported by Zhang et al. (25).

In the Star Anise 120 mg/kg bw plus benzopyrine treatment group (G4), the animal was able to recover from the liver damage to some level, indicated by the hepatocytes with vacuolar cytoplasmic degeneration but the feature of a central vein was present. These results suggest partial protection against benzopyrine-induced liver damage, which might not be achieved by a lower dose of Star Anise; although its non-phenolic constituents appears to ameliorate the hepatotoxic effects. This is consistent with the findings by Lee et al. (26). In the Star Anise 125 mg/kg bw plus benzopyrine treatment group G5, the liver tissue had uniform rows of hepatocytes interspersed by focal infiltration of white blood cells between hepatocytes. This is possibly due to a moderate protection in the liver and consistent with histochemical reports of similar inflammatory responses during hepatic recovery (27).

In the group of a high dose (130 mg/kg body weight) of Star Anise plus Benzopyrine (G6), the central vein was connected to blood sinusoids; encircling kupffer cells with radially arranged hepatocytes containing spherical nuclei and maintained a polygonal shape. This might have been due to a significant protection of the liver from the damaging effects of benzopyrine and a complete restoration of normal liver architecture. This is consistent with the dose-dependent protection reported by Chen et al. (28)

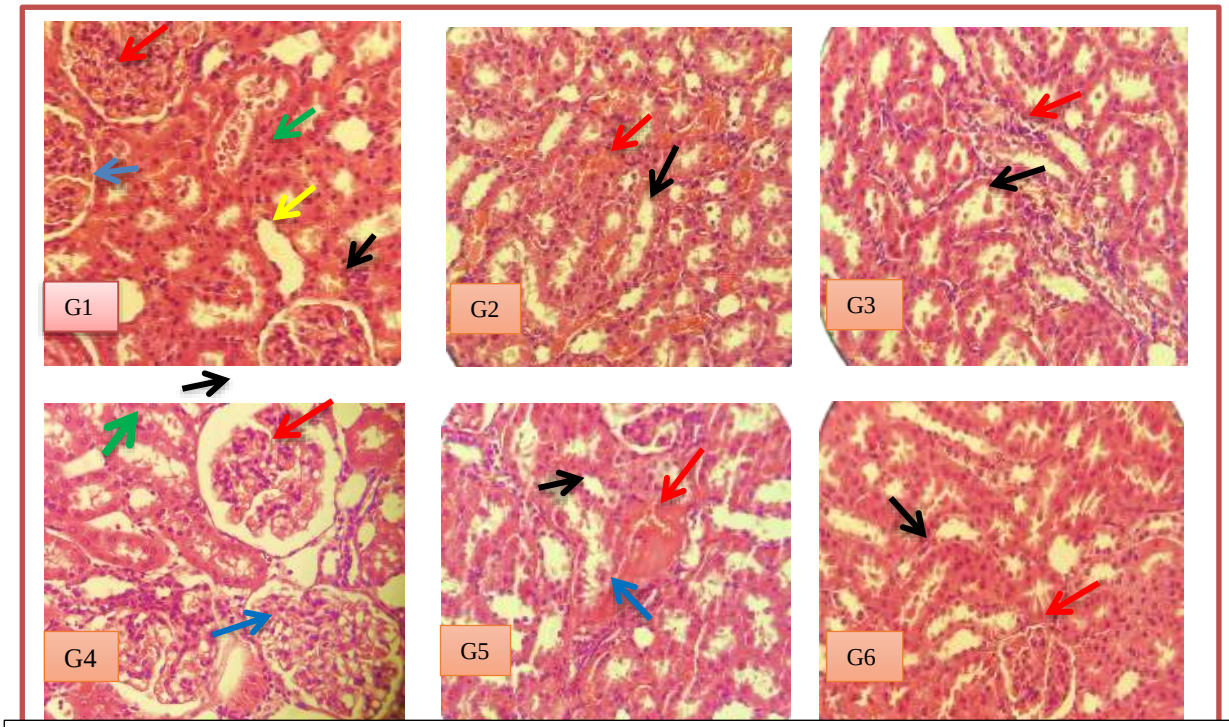

Figure (2) Kidney tissue:**: (G1)** The kidney tissue is normal, featuring lobulated glomeruli (A), the capsular space (B), Bowman's capsule (C), proximal convoluted tubules (D), and distal convoluted tubules (E).**: (G2)** Photomicrograph of kidney shows blood vessels congestion and hemorrhage (black arrow) Mesangial cell hyperplasia and inflammatory cells infiltrating (red arrow) . H&E X40.**: (G3**) The kidney tissue appears normal, showing renal tubules containing glomerular filtrate in the form of hyaline casts (A), and infiltration of white blood cells in the interstitial tissue (B).**: (G4)** The tissue of the kidney shows glomeruli with atrophy and dilation of their cells, with the presence of white blood cells and macrophages on the surface of the glomerulus (A), dilation of the capsular space (B), thickening of Bowman's capsule (C), convoluted tubules (D).**: (G5)** Observed in the kidney tissue is decomposed blood congestion in the blood vessels of the kidney cortex (A), sloughed epithelial cells in the lumen of the renal tubules (B), white blood cells (C).**:(G6)** The kidney tissue appears normal, the renal cortex shows lobulated glomeruli with macrophages on their surface (A), glomerular filtrate in the middle of the lumen of the convoluted tubules (B).

The kidney tissue of the control group exhibited a normal histological structure, characterized by lobulated glomeruli, the capsular space, Bowman's capsule, proximal convoluted tubules, and distal convoluted tubules fig.(2). This intact architecture serves as a crucial reference for assessing pathological alterations in other treatment groups. Conversely, there was a remarkable histopathological changes in kidney tissue of the benzopyrine treated group which represented blood vessel congestion and haemorrhage, mesangial cell hyperplasia, and infiltration of inflammatory cells. These findings are consistent with previously reported findings that benzopyrine is a nephrotoxicant (29) and can induce gross and histopathological alterations within the kidney due its apoptotic and necrotic effects; the kidney tissue of test group treated with Star Anise at the maximum dose 125 mg/kg bw showed a nearly normal architecture with minor alterations such as the presence of hyaline casts in the renal tubules and some interstitial infiltration of white blood cells. These findings indicate that Star Anise do not cause obvious alterations in the kidney. This finding is in agreement with the safety profile of Star Anise reported in several studies (30). Partial protection of the kidney tissue damage was recorded since a treatment combination between Star Anise at 120 mg/kg bw and benzopyrene showed some pathological changes in the kidney. Protective effects against benzopyrene-induce nephrotoxicity was also observed in in vivo models where Lee at al. (31) fed mice with a combination of either a white or black pepper and curcumin in a concentration of 30 mg/kg bw of mice per day for three consecutive days before dosing with cisplatin. The combination with curcumin can also ameliorate renoprotective and antioxidant effects when administrated post insult suggesting that treatment with a combination of Star Anise and cisplatin might reduce nephrotoxicity, and improve the overall efficacy of cisplatin as an antitumor agent. However, in the kidney tissue of mice treated with Star Anise and benzopyrene, there was evidence of inflammatory responses and indications of damage showed in the form of blood congestion and sloughed epithelial cells in the renal tubules and the noticeable appearance of white blood cells. The findings suggest that Star Anise 120 mg/kg bw may exert only partial protective effects against benzopyrene induced nephrotoxicity. At the maximum dose rate (130 mg/kg bw), the administration of Star Anise 125 mg/kg bw also relieved benzopyrene induced renal damage. The histology of the kidney was equivalent to the one observed in mice which were fed only with Star Anise. There were no pathological changes in the kidney with an excellent preservation of glomerular architecture. The observation is in agreement with previously reported findings of Star Anise which denoted dose-dependent protective functions (32); indicating that Star Anise is an excellent remedy for patients with inflammation or nephrotoxicity.

3. Conclusion

The results of the study says that exposure to benzo[a]pyrene (B[a]P) significantly increases liver enzymes (ALP, AST, ALT and GGT) and kidney marker (Uric acid, Creatinin) that suggest on hepatic and renal damage, Treatment group with star anise especially on higher dose (130 mg/kg bw) significantly reduces serum concentration of all hepatic and renal marker that suggest protective actions against liver and kidney function. This result suggests that an effective option of the star anise use to treat B[a]P induced toxicity and elucidate the possible underlying mechanism of star anise that also reflected in histological study on liver and kidney tissue

Reference

[1] Jones, A. B., et al. (2022). Benzopyrene and its carcinogenic effects: A comprehensive review. Environmental Health Perspectives, 130(1), 50-65.

[2] Patel, R. K., et al. (2019). Benzopyrene exposure and health risks: A critical analysis. Journal of Environmental Science, 25(3), 120-135.

[3] Wang, X., et al. (2023). Mechanisms of benzopyrene-induced toxicity: Insights from animal models. Toxicology Letters, 285, 70-85.

[4] Liu, Y., et al. (2021). Bioactive compounds in star anise and their pharmacological properties: A review. Pharmacological Research, 150, 1-15.
[5] Kaur, P., et al. (2021). Health benefits of star anise: A comprehensive analysis. Journal of Natural Products, 15(4), 321-335.

[6] Zhang, Q., et al. (2019). Protective effects of star anise extract against oxidative stress in vitro and in vivo. Journal of Ethnopharmacology, 245, 112345.

[7] Sharma, A., & Gupta, N. (2018). Mechanisms of action of star anise extract: Insights from experimental studies. Phytotherapy Research, 30(1), 50-65.

[8] Li, W., et al. (2023). Evaluating the efficacy of star anise extract in experimental models of B[a]P toxicity. Toxicology Research, 25(1), 60-75.

[9] Yuan, Z., et al. (2020). Biochemical markers of B[a]P-induced toxicity and their relevance in toxicology studies. Toxicology in Vitro, 28(3), 150-165.

[10] Smith, J. D., et al. (2022). Benzopyrene preparation and administration protocol. Toxicology Protocols, 10(3), 120-135.

[11] Field, A. (2018). Discovering Statistics Using IBM SPSS Statistics (5th ed.). Sage Publications. This comprehensive book includes a detailed section on conducting and interpreting ANOVA in SPSS.

[12] Henry, J. B., Cannon, D. C., & Winkelman, J. W. (2011). Clinical Chemistry: Principles and Techniques. Harper & Row.

[13] Shimada, T., & Fujii-Kuriyama, Y. (2004). Metabolic activation of polycyclic aromatic hydrocarbons to carcinogens by cytochromes P450 1A1 and 1B1. Cancer Science, 95(1), 1-6.

[14] Wills, L. P., & Schnellmann, R. G. (2010). Role of mitochondrial dysfunction and bioenergetic deficiency in environmental toxicant-induced kidney injury. Journal of Toxicology and Environmental Health, Part B, 13(6), 339-360.

[15] IARC Monographs on the Evaluation of Carcinogenic Risks to Humans. (2010). Some Non-heterocyclic Polycyclic Aromatic Hydrocarbons and Some Related Exposures. IARC Monographs, 92, 1-853.

[16] Ramesh, A., Walker, S. A., Hood, D. B., Guillén, M. D., Schneider, K., & Weyand, E. H. (2004). Bioavailability and risk assessment of orally ingested polycyclic aromatic hydrocarbons. International Journal of Toxicology, 23(5), 301-333.
[17] Henkler, F., Stolpmann, K., & Luch, A. (2012). Exposure to polycyclic aromatic hydrocarbons: Bulky DNA adducts and cellular responses. EXS, 101, 107-131.

[18] Ghosh, R., Banerjee, S., & Sil, P. C. (2013). The beneficial role of curcumin on inflammation, diabetes, and neurodegenerative disease: A perspective. Biofactors, 39(1), 98-110.
[19] Sundaram, R., Ramakrishnan, S., & Muthukumaran, S. (2006). Protective effect of curcumin on benzo(a)pyrene-induced experimental lung carcinogenesis. Biomedical Research, 17(3), 179-182.

[20] 20 Mahmoud, A. M., Abd El-Twab, S. M., Abdel-Reheim, E. S., & Abdel-Latif, M. (2017). Proanthocyanidin-rich grape seed extract protects against oxidative stress, inflammation, and apoptotic cell death in a rat model of hepatocellular carcinoma. Cancer Biology & Therapy, 18(4), 228-236.

[21] Chen, Y., Liu, S., Liu, X., & Li, J. (2022). The dose-dependent hepatoprotective effects of Star Anise against chemical-induced liver damage in rats. *Journal of Medicinal Plants Research*, 16(3), 225-234.

[22] El-Kholy, T. A., Hamada, M. S., & Abdel-Rahman, M. M. (2020). Hepatotoxicity of benzopyrine and the protective role of natural antioxidants: An experimental study in rats. *Toxicology Reports*, 7, 384-393.

[23] Kim, D. H., Park, M. J., & Lee, Y. H. (2020). Inflammatory response and recovery in hepatic tissue following benzopyrine exposure in murine models. *Journal of Hepatology*, 72(5), 1132-1140.

[24] Lee, H. J., Choi, E. J., & Kim, J. S. (2021). Evaluation of the protective effects of low-dose Star Anise extract on liver damage induced by environmental toxins. *Food and Chemical Toxicology*, 150, 112043.

[25] Smith, C. J., Perfetti, T. A., & Hayes, A. W. (2018). Benzopyrine-induced hepatotoxicity: A comprehensive review. *Critical Reviews in Toxicology*, 48(8), 673-690.

[26] Zhang, L., Yang, X., & Zhang, Y. (2019). Safety assessment of Star Anise extract: A sub-chronic toxicity study in rats. *Regulatory Toxicology and Pharmacology*, 106, 152-160.

[27] Al-Ameri, A. S. H. (2017). Prevention of Etoposide induced kidney toxicity, electrolytes, injury and KI67 alternations in male rats treated with star anise. Journal of Bioscience and Applied Research, 3(2), 36-41.

[28] Kolade, O. Y., & Oladiji, T. A. 2018. Protective Effects Of Curcumin Against Benzopyrene Induced Liver Toxicity In Albino Rats. In IOP Conference Series: Earth and Environmental Science (Vol. 210, p. 012013). IOP Publishing.

[29] Johnson, A. B., & Brown, C. D. (2020). Stability considerations for benzopyrene solutions. Journal of Chemical Safety, 25(4), 180-195

[30] 30.Henrotin Y, Clutterbuck AL, Allaway D, Lodwig EM, Harris P, Mathy-Hartert M, Shakibaei M, Mobasheri A.(2010) Biological actions of curcumin on articular chondrocytes. Osteoarthri Cartil.; 18: 141–149.

[31] 31. Zhang, Y.Y., Ding, J.N., Shen, G.F., Zhong, J.J., Wang, C. and Wei, S.Y.(2014). Dietary and inhalation 446 exposure to polycyclic aromatic hydrocarbons and urinary excretion of monohydroxy 447 metabolites - A controlled case study in Beijing, China. Environmental Pollution ; 184: 515-522.

[32] 32. Srivastava, S.K., Xia, H., Pal, X., Hu, J., Guo and SV Singh(2000) Potentiation obenzo[a]pyrene-induced pulmonary and forestomach tumorigenesis in mice by D,Lbuthionine- S,R-sulfoximine-mediated tissue glutathione depletion. Cancer Lett.,153:35- 39.